ELSEVIER

Nuclear Instruments and Methods in Physics Research A 447 (2000) 424–431

NUCLEAR INSTRUMENTS & METHODS IN PHYSICS RESEARCH Section A

www.elsevier.nl/locate/nima

Response to cosmic rays of the large-angle electromagnetic shower calorimeter of the CLAS detector

M. Anghinolfi[a], M. Battaglieri[a], P. Corvisiero[a], R. De Vita[a], E. Golovach[a,1], A. Longhi[a,2], V. Mokeev[a,1], G. Ricco[a], M. Ripani[a], V. Sapunenko[a,1], M. Taiuti[a,*], H. Avakian[b], N. Bianchi[b], E. De Sanctis[b], V. Gyuriyan[b,3], V. Muccifora[b], M. Mirazita[b], E. Polli[b], A.R. Reolon[b], F. Ronchetti[b], P. Rossi[b]

[a] *Dipartimento di Fisica dell'Università di Genova or Istituto Nazionale di Fisica Nucleare, Sezione di Genova, I-16146 Genova, Italy*
[b] *Istituto Nazionale di Fisica Nucleare, Laboratori Nazionali di Frascati, 00044 Frascati, Italy*

Received 1 November 1999; received in revised form 26 November 1999; accepted 2 December 1999

Abstract

The measurement of the response of the large-angle electromagnetic shower calorimeter (LAC) of the CLAS detector to minimum ionizing particles is reported. The experimental set-up and the adopted procedures are described. The results of the light attenuation length in the calorimeter, the light output and the resolution of the interaction point reconstruction are discussed. The performances of the LAC match well with those required. © 2000 Elsevier Science B.V. All rights reserved.

PACS: 29.40.Vj

Keywords: Electromagnetic shower calorimeter; Response to minimum ionizing particles

1. Introduction

The AIACE collaboration [1] participates in the TJNAF (formerly CEBAF) [2] Hall B experimental activity. Hall B is equipped with the Large Acceptance Spectrometer CLAS [3] based on a toroidal magnetic field produced by six superconducting coils arranged around the beam line. Each region between the two coils acts as a single spectrometer equipped with three layers of drift chambers for track reconstruction, one layer of scintillator counters for time-of-flight measurement, a Cherenkov detector and an electromagnetic shower calorimeter. The forward calorimeter modules cover the polar scattering angle θ interval from 10° to 45° in the laboratory frame in all the six sectors. The two LAC modules realized by the AIACE collaboration extend the θ coverage up to 75° in two CLAS sectors.

* Corresponding author. Tel.: 39-010-353-6458; fax: 39-010-313-358.

E-mail address: taiuti@ge.infn.it (M. Taiuti).

[1] Permanent address: Institute of Nuclear Physics, Moscow State University, 119899 Moscow, Russia.

[2] Present address: The Catholic University of America, Washington, DC 20064, USA.

[3] Present address: Thomas Jefferson National Accelerator Facility, Newport News, VA 23606, USA.

PII: S0168-9002(99)01287-5

This paper, after a description of the LAC detector, reports on the results of several tests performed with cosmic rays both at Costruzioni Saldate Collaudate (C.S.C.) Workshop in Schio (Italy) where the modules were assembled and later at TJNAF after transportation and insertion in the CLAS detector. Both energy and timing response to minimum ionizing particles were studied for the two modules. In particular, the light propagation in scintillators, the number of photoelectrons/MeV collected, and the position reconstruction resolution were measured. The measurement was crucial to verify that the calorimeter response meets the design specifications, considering the fact that at that time new scintillating material and light collecting system were used. The tests showed that the module properties well agree with the initial specifications.

2. Detector description

A conceptual drawing of an LAC module and its internal structure is shown in Fig. 1. The modules have a multi-layer structure with lead sheets and scintillator bars, a configuration that provides the best compromise between good energy resolution and high neutron detection efficiency. Each module consists of 33 layers, each composed of a 0.20 cm thick lead foil and NE110A plastic scintillator bars roughly by 10 cm width and a constant thickness of 1.5 cm [4,5]. The bar width increases going from the inner toward the outer side to guarantee the tapering required by the CLAS geometry. The module thickness corresponds to 12.9 radiation lengths and 1.0 absorption length. Teflon sheets 0.2 mm thickness separate scintillators from lead and 0.2 mm thick Teflon strips between each pair of contiguous scintillator bars avoid optical cross-over. In each layer scintillators are oriented along the same direction; in consecutive layers they are rotated by 90° one respect to the other to form a 40×24 matrix of rough $10 \times 10\,\mathrm{cm}^2$ cells. The surface of the module exposed to particle fluxes is $217 \times 400\,\mathrm{cm}^2$. The module is vertically divided into an inner (17 layers) and an outer (16 layers) parts with separate light readouts to improve the electron–pion discrimination [6]. Scintillators

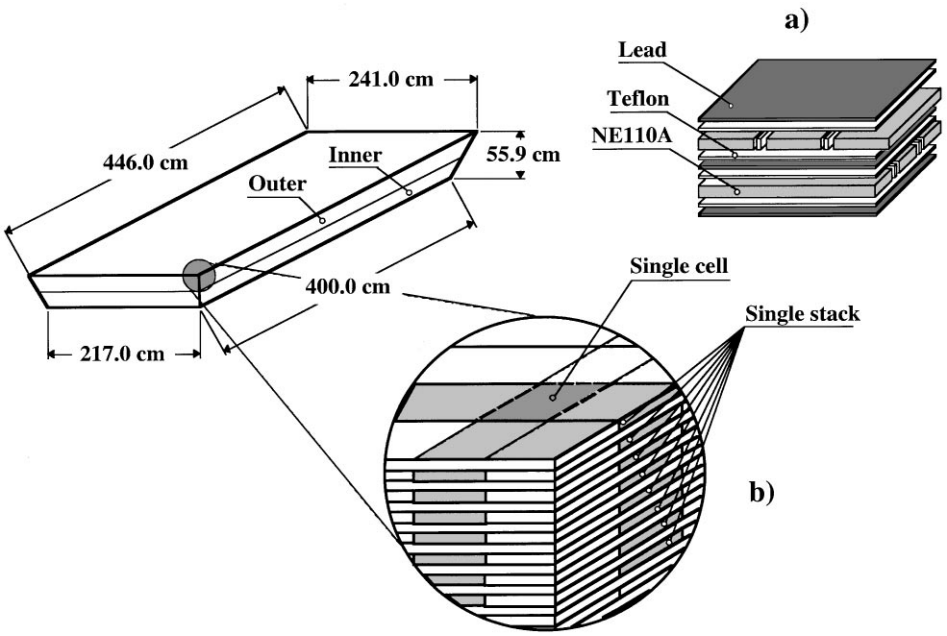

Fig. 1. Conceptual drawing of an LAC module showing in detail: (a) the composite internal structure and (b) the plastic scintillators stack structure (light-gray area) with the crossing of two orthogonal stacks that defines a cell (dark-gray area).

lying (for the inner and outer part separately) one on top of the other with the same orientation form a stack. For each module there are 128 different stacks.

Electromagnetic showers originate in the lead sheets and propagate through the layers; the energy absorbed in the active material produces a light pulse that is collected at both scintillator ends with Lucite light guides coupled to scintillators via an air gap [7]. As the coupling area ($7.0 \times 0.4\ cm^2$) is smaller than the scintillator cross section, the uncoupled scintillator surface is protected with a Teflon sheet to prevent scratches from the aluminum external structure. To reduce photocathode nonhomogeneity effects, the light guides are glued together before being coupled to the photomultiplier. Scintillators forming a stack are coupled at the two bar ends to different EMI 9954A photomultipliers placed above the top surface of the LAC module as shown in Fig. 2. Then, each module is equipped with 256 photomultipliers.

Monte Carlo simulations [8,9] showed that the LAC performances are strongly affected by the efficiency of light transmission and collection. For this reason special attention was devoted to the quality of scintillators, light guides and photomultipliers whose performances have already been reported in previous papers [5,7,10]: in particular, scintillators with a light attenuation length longer than 300 cm and light guides with good light transmission were selected in order to have about 5 photoelectrons/MeV at the photomultiplier anodes. The amount of the collected light inhomogeneities among scintillators, light guides, and photomultipliers were reduced, (a) by sorting the scintillators from center toward the borders as a function of decreasing attenuation length and (b) coupling the best scintillators-light-guide groups to the worst photomultipliers, and vice versa.

The photomultiplier signal is first split right after the base output: a prompt signal provides the trigger, the other, through a 470 ns low attenuation

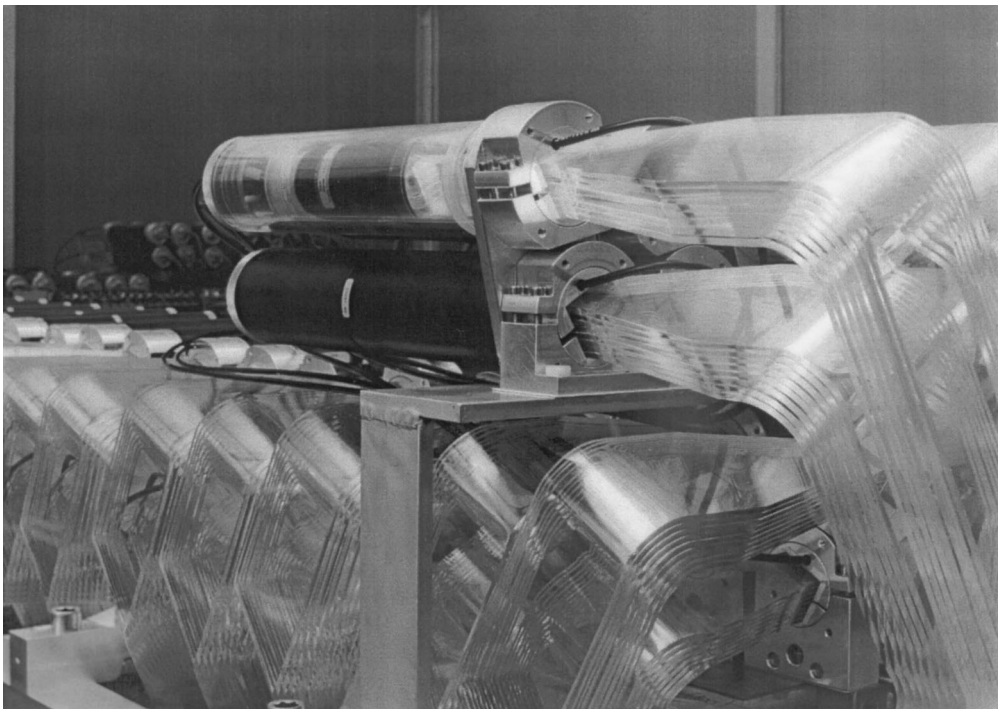

Fig. 2. Picture of the LAC Light Readout System (LRS) showing the coupling to photomultipliers taken during the first module construction. One of the photomultiplier housings has been replaced with a Plexiglas tube to show the LRS coupling to photocathode.

RG8 delay cable, goes through a resistive splitter that provides two equal signals to the CAEN C222 CAMAC discriminators and the LeCroy LC1881M FASTBUS ADC. The discriminator outputs provide the stop signals to the LeCroy LC1875A FASTBUS TDC. Considering that (a) the maximum released energy in a single stack in experiment is, from Monte Carlo simulations, of about 350 MeV, (b) the pulse shape is approximately triangular with about 20 ns base, (c) the discriminator minimum threshold is 15 mV, and (d) the ADC range is 0–400 pC, the proposed splitter permits to cover the full ADC range with the minimum 3 MeV detected energy in discriminators necessary for neutron detection.

To perform the cosmic-ray measurements the module projecting geometry was used. The prompt OR'ed signal from all 256 photomultipliers was used as the trigger and the cosmic muons crossing the module through a single cell were selected off line. In addition, C.S.C. measurements were also performed placing the module horizontally and in coincidence with a $10 \times 10 \times 2\,\mathrm{cm}^3$ plastic scintillator placed in the detector focus above the detector itself. In this configuration a cosmic muon hitting the coincidence scintillator crossed the calorimeter mostly through a single cell.

3. The energy resolution

The single-cell energy deposition spectra were selected, in the off-line analysis, by imposing the presence of four ADC signals in the inner part and of the four corresponding ADC signals in the outer part of the detector. Fitting the energy spectra to Gaussian functions, for each photomultiplier two plots were produced giving the position dependence of mean and sigma of the deposited energy. Fig. 3 shows a typical dependence on the cell coordinate of the mean readout charge; after correcting for the deposited energy due to the different effective thickness of the cells, the light transmission function is well described by two exponentials:

$$Q(x) = Q_0(\mathrm{e}^{-x/\lambda} + \alpha \mathrm{e}^{-(2L-x)/\lambda}). \quad (1)$$

The first exponential describes the attenuation of the light though the scintillator and the second one

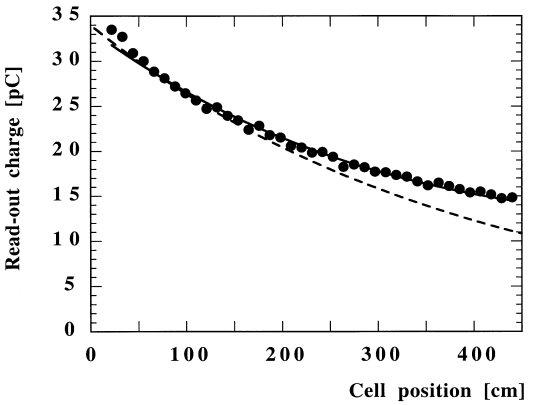

Fig. 3. Typical dependence on the cell coordinate of the mean readout charge. Continuous line represents the best exponential fit taking into account light reflection at the opposite end of the scintillator bars, the dashed line shows the contribution of direct light only. Errors on experimental points are smaller than the symbol size.

originates from the light reflection on the opposite end of the scintillator. This effect, being the attenuation length values comparable to the bar length, is enhanced by the Teflon tape placed on both scintillator ends. It was clearly visible observing the photomultiplier pulses at the oscilloscope. In Eq. (1) α represents the reflection coefficient, λ is the average attenuation length obtained from the measured values for the scintillators belonging to the stack [5], and L is the stack length. The solid line in Fig. 3 represents a fit to the form in Eq. (1). For comparison the dashed line shows the contribution of the directly transmitted light ($\alpha = 0$): a contribution of the reflected light, of up to about 40%, clearly emerges from the comparison between the two curves.

Fig. 4 shows a typical position dependence of the relative sigma of the deposited energy distribution in a single stack: the value slowly increases as a function of the distance of the cell from the photomultiplier. There are two contributions: (a) the Landau fluctuations σ_L/E_d provide a constant contribution, estimated from Monte Carlo simulations equal to 10.5% and 11.5% in the two trigger configurations at C.S.C. and TJNAF, respectively, and (b) the fluctuations in the light collection statistics, which is proportional to the deposited energy and to the stack light transmission properties. The

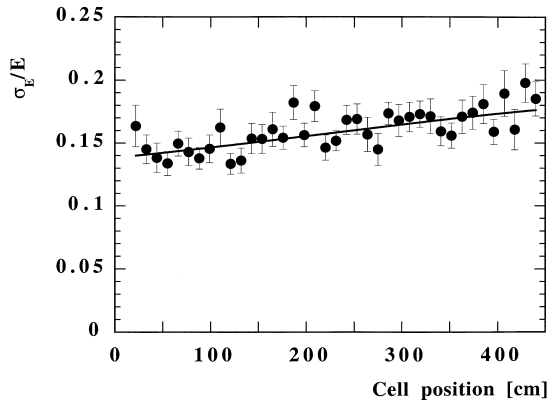

Fig. 4. Typical dependence on the cell coordinate of the relative width σ_E/E of readout energy distribution. The continuous line represents the best fit taking into account the intrinsic Landau width and the collected photoelectron fluctuations.

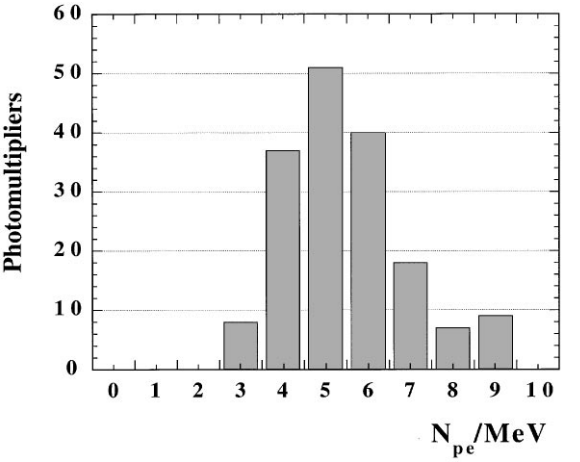

Fig. 5. Distribution of the number of photoelectrons/MeV collected at photomultiplier coupled to the long scintillator bars.

solid line in Fig. 4 represents the fit with these two contributions quadratically summed using the expression

$$F(x) = \left(\left(\frac{\sigma_L}{E_d}\right)^2 + \frac{1}{N_{p.e.}E_d(e^{-x/\lambda} + \alpha e^{-(2L-x)/\lambda})}\right)^{1/2} \quad (2)$$

where $N_{p.e.}$ is the number of photoelectrons/MeV and $E_d \approx 25$ MeV the average deposited energy in one stack. The extraction of $N_{p.e.}$ from the fit resulted more effective in the case of long stacks where the x dependence of the fluctuations of transmitted light statistics is more prominent.

A summary of the obtained $N_{p.e.}$ for the two modules is reported in Fig. 5 for long scintillator bars. The rms value of the distributions, equal to 23%, is comparable with the convolution of those measured for single scintillators, light guides and photomultipliers, while the average value $N_{p.e.} = 5$ is equal to the value resulting from Monte Carlo simulations.

Considering the average measured light output for single scintillator (59 photoelectrons/MeV [5]), it results that the attenuation factor in light guides is about 12 in agreement with that measured during the light-guide acceptance tests. This value is larger than the value 8 reported in Ref. [7] because the final light guides are longer than the design ones and with a third bending to fit the module geometry.

The dependence in Eq. (1) of the energy read-out on the cell position is used to efficiently reconstruct the actual deposited energy, independent of the impact point. The combined signal

$$Q_C(x) = (Q_{Left}(x)Q_{Right}(x))^{1/2} \quad (3)$$

from the read-out charge Q_{Left} and Q_{Right} of the two photomultipliers coupled to a single stack is almost unaffected by the muon crossing point x. In Fig. 6 a typical position dependence of the average values for $\langle Q_C(x)\rangle$, $\langle Q_{Left}(x)\rangle$ and $\langle Q_{Right}(x)\rangle$ in one stack are reported: $\langle Q_C(x)\rangle$ is almost flat (within $\pm 4\%$) with a small rising close to the stack edges, while $\langle Q_{Left}(x)\rangle$ and $\langle Q_{Right}(x)\rangle$ show the exponential behavior described above. In Fig. 7 the $\langle Q_C(x)\rangle$ distribution measured for the long stacks of the two modules is shown: the centroid of the distribution is 24.8 ± 0.9 pC.

When all cells are taken into account, $Q_C(x)$ provides, the energy distribution for muons for the LAC module as reported in Fig. 8: the plot has been obtained by summing, for each detected particle, the deposited energy in the four stacks. The central value of the distribution is 106 MeV $\pm 9.5\%$ well in agreement with the Monte Carlo simulations.

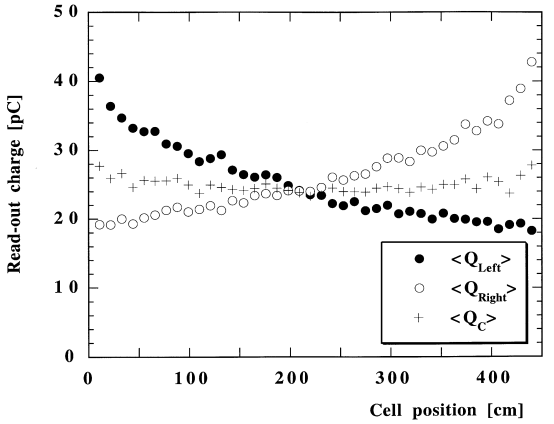

Fig. 6. Position compensation for collected charge from a single stack as described in the text.

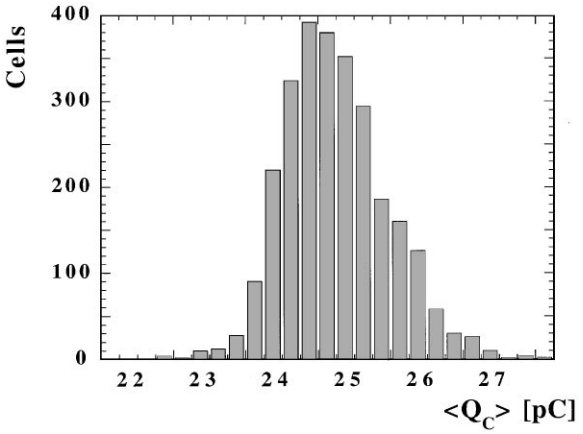

Fig. 7. Distribution of $\langle Q_C \rangle$ for the long stacks of the two modules.

4. The timing resolution

The timing properties of the LAC modules were also determined by studying the effect of the fluctuations of the position reconstruction. With the same criteria adopted to select deposited energy in a single cell, single-cell timing distributions were measured for the half-difference

$$\Delta t = \tfrac{1}{2}\,(t'_{\mathrm{Left}} - t'_{\mathrm{Right}}) \tag{4}$$

and for the half-sum

$$\sum t = \tfrac{1}{2}\,(t'_{\mathrm{Left}} + t'_{\mathrm{Right}}) \tag{5}$$

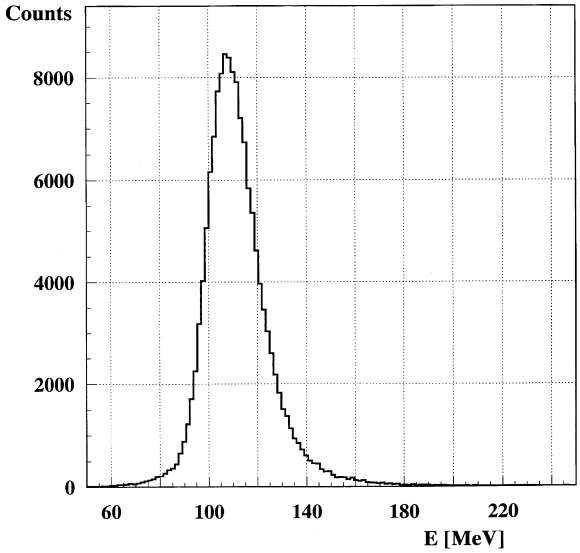

Fig. 8. Deposited energy for muons.

obtained from the TDC responses t_{Left} and t_{Right} of the two photomultipliers coupled to opposite ends of the same stack corrected, as discussed in Ref. [7], for the time walk with the function

$$t' = t - 3.79\mathrm{e}^{-Q/28} \quad [\mathrm{ns}] \tag{6}$$

being Q the read-out charge in pC. Fitting the timing spectra with Gaussian functions for each pair of photomultipliers and for each cell the mean $\langle \Delta t \rangle$ was evaluated. From the position dependence of $\langle \Delta t \rangle$ the velocity of light v in the stack was extracted. The values 16.0 ± 0.3 cm/ns for the mean and rms distribution well agree with those measured in single scintillators [5].

Good timing resolution is required to extract the momentum of the detected neutron from the impact point in the LAC and time of flight from target and LAC. In particular, Δt permits to reconstruct the impact point of those neutrons that, interacting in only one scintillator bar, have no x–y readout. However, in the cosmic rays tests discussed in this paper, Δt cannot provide a precise value of the detector timing being dominated by the cell size. This can be clearly seen in Fig. 9 where the difference between the reconstructed impact point and the center-of-cell coordinate has been reported for all cells.

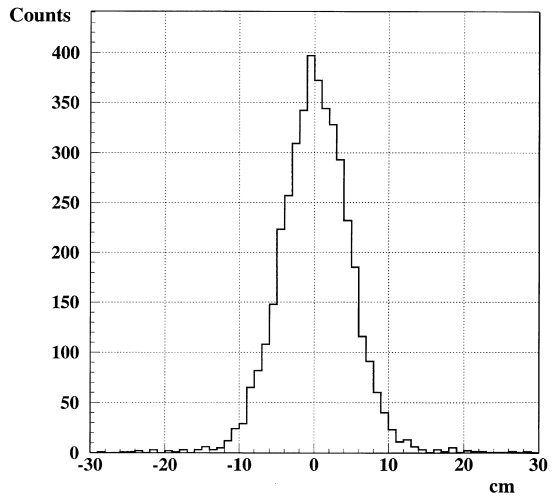

Fig. 9. Distribution of the difference between the reconstructed impact point in short stacks and the center-of-cell coordinate.

The central value of the distribution is 0.0 ± 4.3 cm. The comparison with the Monte Carlo calculation, 0.0 ± 3.8 cm, shows that the timing fluctuation gives a ± 2.0 cm uncertainty to the position reconstruction.

A much better estimate of the timing resolution was obtained from Σt. In the measurements performed at C.S.C. each detected muon crosses the trigger detector and four stacks in the calorimeter. The difference between Σt values obtained with different stacks does not depend on the muon impact point and the trigger detector timing uncertainties. Fig. 10 shows the overall results for short and long stacks from the module inner part: the distribution is gaussian with $\sigma = 270$ ps. Comparable results have been obtained with all other stack combinations.

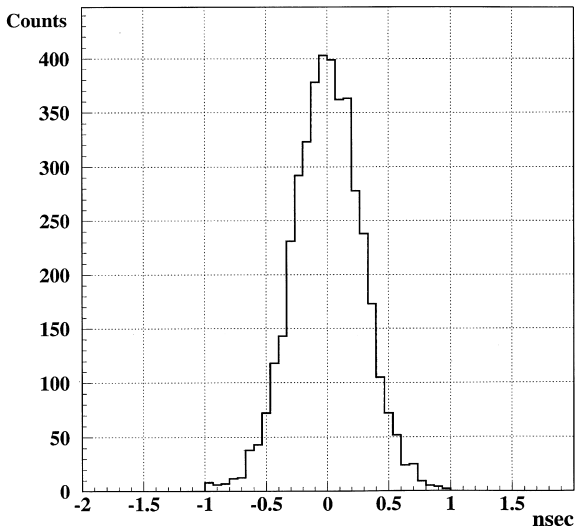

Fig. 10. Distribution of the difference between Σt from long and short stacks of the inner part of the first module.

5. Conclusions

The response of the two LAC modules of the CLAS detector to minimum ionizing particles has been studied considering the contribution of light propagation and collection efficiency. The light output, the light transmission, and the timing selecting only the particles that crossed the module through a single cell were measured. The measurements were performed several times over a two year period showing no significant variations in the detector response.

The measurements showed that the module performances match well with those expected by simulations.

Acknowledgements

We thank dr. F. Anselmi for the support provided at C.S.C., the INFN Frascati and Genova technical staffs, M. Albicocco, P. Cocconi, A. Orlandi, F. Parodi, W. Pesci, A. Rottura, G. Serafini and A. Viticchiè for the continuing assistance during the measurements, and the TJNAF Laboratory for the support provided during the installation and test of the two modules.

References

[1] M. Anghinolfi et al., in: F. Balestra, R. Bertini, R. Garfagnini (Eds.), Proceedings of the International Workshop on Flavour and Spin in Hadronic and Electromagnetic Interactions, Torino September 21–23, 1992, Vol. 39, Italian Physical Society, 1993, p. 237.

[2] J.J. Domingo, in: S. Boffi, C. Ciofi degli Atti, M. Giannini (Eds.), Proceedings of the fifth Workshop on Perspectives in Nuclear Physics at Intermediate Energies, Trieste May 6–10, 1991, World Scientific, Singapore, 1992, p. 260.
[3] V.D. Burkert, B.A. Mecking, in: B. Frois, I. Sick (Eds.), Modern Topics in Electron Scattering, World Scientific, Singapore, 1991.
[4] M. Taiuti et al., Nucl. Instr. and Meth. A 357 (1995) 344.
[5] P. Rossi et al., Nucl. Instr. and Meth. A 381 (1996) 32.
[6] M. Taiuti et al., INFN Report INFN-GE/BE-95-03.
[7] M. Taiuti et al., Nucl. Instr. and Meth. A 370 (1996) 429.
[8] V.I. Mokeev et al., INFN Report INFN-GE/BE-95-02.
[9] M. Taiuti, Proceedings of the Sixth International Conference on Calorimetry in HEP, Frascati, June 8–14, 1996, Frascati Physics Series, 1996, p. 201.
[10] M. Ripani et al., Nucl. Instr. and Meth. A 406 (1998) 403.